Impact of transmitter wavefront errors and pointing jitter on intersatellite free space optical communications

Badas Aldecocea, M.; Bouwmeester, J.; Piron, P.; Loicq, J.J.D.

DOI
10.1117/12.3021617

Publication date
2024

Document Version
Final published version

Published in
SPIE Optical System Design 2024

Impact of transmitter wavefront errors and pointing jitter on intersatellite free space optical communications

Mario Badás Aldecocea[a], Jasper Bouwmeester[a], Pierre Piron[a], and Jérôme Loicq[a,b]

[a]Department of Space Engineering, Delft University of Technology, Kluyverweg 1, 2629 HS Delft, Netherlands
[b]Centre Spatial de Liège, University of Liège, Avenue du Pré Aily, 4031 Liège, Belgium

ABSTRACT

Intersatellite optical communication links will be crucial for the development of future global optical and quantum communication networks. Under the harsh space environment satellite optical terminals will suffer pointing jitter and wavefront errors. In this paper, the impact of the combination of these errors on the transmitter side is modeled. Combining the far-field diffraction patterns obtained through computational Fourier optics and the statistics of the pointing jitter, the received power statistics are derived numerically for different scenarios. The computational model is first used to evaluate the optimum nominal parameters of the transmitted beam. Then, several optical aberrations are added to the transmitted beam and their impact on the communication performance is evaluated through the average bit error rate.

Keywords: free space optical communications, satellite communication, wavefront errors, optical aberrations, Fourier optics, far-field diffraction, Gaussian beam

1. INTRODUCTION

The backbone of global communication networks highly depends on the intersatellite links that compose these. However, the technology has to be updated for the higher data transmission and security requirements demanded by society. Most of the current intersatellite communication links are based on radiofrequency technologies. Free Space Optical Communication (FSOC) links use higher frequencies of the electromagnetic spectrum for the carrier beam, allowing higher data rates than radiofrequency signals. Furthermore, the high directionality of the laser beams that carry the information in FSOC hinders the interception of the beam, making it a more secure communication. In addition, intersatellite FSOC links will be a key enabler of the future space-based quantum communication networks.[1–3]

However, several challenges must be overcome when considering an intersatellite FSOC link. The high directionality of the coherent beam also means a high sensitivity to the pointing error of the transmitter (see Figure 1). The pointing error on the transmitter side will deviate the center of the beam from the receiver's optical axis. As the peak irradiance will be located at the center of the beam, the optical power captured by the receiver's aperture will be reduced. The in-orbit sources of the pointing error are diverse[4] and generate a stochastic displacement of the beam in the receiver's aperture plane. On the receiver side, the pointing jitter can also affect the performance of the system. The latter's effects are not considered in this paper.[5]

Furthermore, as with any other optical system in the space environment, intersatellite FSOC terminals will be subjected to wavefront errors. The varying thermal and mechanical loads in space will create deformations of the optical components that will create wavefront errors in the beams traveling through these systems. Although these wavefront errors can occur in every component of the optical system, the primary mirror of the telescope will be one of the most affected. This is due to its bigger size and the higher exposition to the space thermal environment compared to the rest of the components. In the following, the effects of the transmitter wavefront error are considered as if this wavefront error were being applied in the aperture plane of the transmitter. The wavefront errors can also have a detrimental impact on the communication performance of FSOC links. Indeed,

Further author information: (Send correspondence to M.B.A.)
M.B.A.: E-mail: m.badasaldecocea@tudelft.nl

Computational Optics 2024, edited by Daniel G. Smith, Andreas Erdmann, Proc. of SPIE
Vol. 13023, 1302302 · © 2024 SPIE · 0277-786X · doi: 10.1117/12.3021617

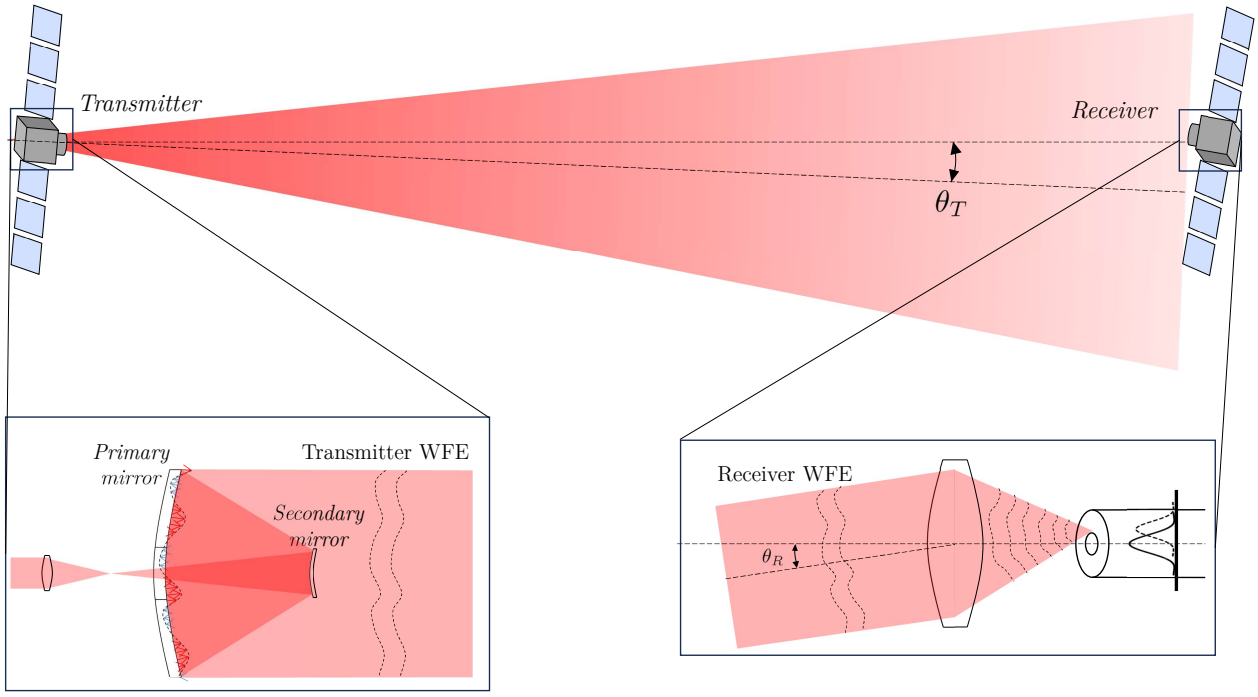

Figure 1. Illustration of the effect of the transmitter and receiver wavefront errors and pointing jitters. θ_T and θ_R represent the transmitter and receiver pointing error at a certain instant of time, respectively.

the far-field irradiance distribution is affected by these errors, and that, will modify the performance of the link from the nominal case. Furthermore, wavefront errors in the receiver terminal also affect the performance of the system, especially when the incoming light is coupled into fiber (see Figure 1).[6]

The analysis of the combined effect of transmitter pointing error and wavefront error is crucial for setting the requirements and ensuring the correct performance of the future satellite FSOC terminals. Previous work has been done modeling the effects of wavefront error and/or pointing jitter in intersatellite FSOC links. Many of these works have focused on the impact on the mutual alignment that these wavefront errors have.[7–11] Other works have focused on the effect of the wavefront errors in the received optical power.[12–14] Finally, there have been a few works analyzing the combined effect of pointing jitter and wavefront error on communication performance.[15,16] However, the latter have not considered the clipping effects due to the secondary and primary mirrors of the transmitter telescope (see Figure 2). In this work, a more realistic model is presented to include the effects of the transmitter and receiver finite-size pupils.

2. NUMERICAL MODEL

In this section, the model to compute the performance of an intersatellite link under transmitter pointing jitter and wavefront errors is presented. First, the computational optical model to obtain the far-field diffraction pattern is presented. Then, the obtained far-field irradiance is combined with the pointing jitter statistics to obtain the statistics of the received power. Finally, the received power is used to compute the communication performance of the intersatellite link.

2.1 Far-field diffraction patterns

In this work the finite aperture of the transmitter is considered, including the effects of the secondary mirror (see Figure 2). To compute the far-field intensity distribution, Fresnel propagation can be numerically evaluated

with[17]

$$U(x,y,z) = \frac{e^{jkz}}{j\lambda z}\, e^{j\frac{k}{2z}\left(x^2+y^2\right)} \int_{-\infty}^{\infty}\int_{-\infty}^{\infty} \left\{U(\xi,\eta,0)\, e^{j\frac{k}{2z}\left(\xi^2+\eta^2\right)}\right\} e^{-j\frac{2\pi}{\lambda z}(x\xi+y\eta)} d\xi d\eta \tag{1}$$

where $U(x,y,z)$ is the field in the receiver aperture plane at a given distance z from the transmitter. The field in the aperture plane of the transmitter is considered to be Gaussian. This beam is clipped by the aperture of the transmitter telescope with pupil function $\mathcal{A}(\xi,\eta)$ (see Figure 2), yielding a field in the transmitter aperture plane given by

$$U(\xi,\eta,0) = U_0\, \frac{w_0}{w(z)}\, \exp\left(-\frac{\xi^2+\eta^2}{w(z)^2}\right) \exp\left(-i\left(kz + k\frac{r^2}{2R(z)} - \nu(z)\right)\right) \mathcal{A}(\xi,\eta) \exp\left[i\, \psi_{\text{WFE}}(\xi,\eta)\right] \tag{2}$$

with

$$\mathcal{A}(\xi,y) = \begin{cases} 1 & \text{if} \quad a \le \sqrt{\xi^2+\eta^2} \le b \\ 0 & \text{else} \end{cases} \tag{3}$$

where $R(z)$ is the radius of curvature of the Gaussian beam wavefront, $\nu(z)$ is the Gouy phase and $\psi_{\text{WFE}}(\xi,\eta)$ is the wavefront error in the transmitter's aperture plane. The bidimensional Fourier transform in Equation 1, can be evaluated numerically using the Fast Fourier Transform. The intensity distribution in the receiver's aperture plane is obtained by simply evaluating $I(x,y,z) = |U(x,y,z)|^2/2\eta_0$ where the wave impedance is $\eta_0 = 377\ \Omega$ for free space. The wavefront error $\phi(\xi,\eta)$ can be expressed in polar coordinates (ρ,φ) using the Zernike polynomials $Z_n^m(\rho,\varphi)$[18]

$$\psi_{\text{WFE}}(\rho,\varphi) = \sum_{n=0}^{\infty}\left(\sum_{m=-n}^{n} a_{nm}\, Z_n^m(\rho,\varphi)\right) \tag{4}$$

where a_{nm} are the coefficients corresponding to the radial index n and the azimuthal index m. Figure 3 shows the first Zernike polynomials along with their classical denominations.

2.2 Received power statistics

The location of the computed far-field intensity distribution in the receiver's aperture plane is affected by the transmitter pointing jitter. This stochastic process will produce received power dynamics, that will degrade the

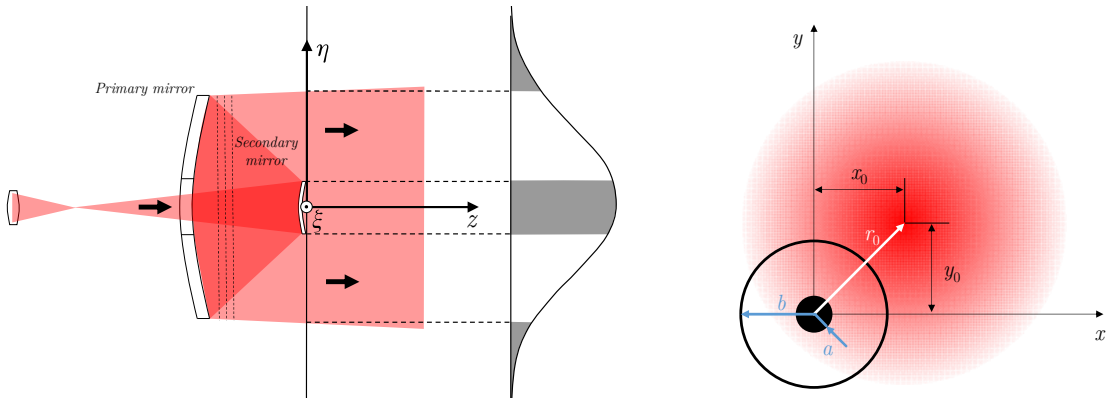

(a) (b)

Figure 2. Clipping and obscuration of the primary and secondary mirrors. (a) transmitter clipping and obscuration and (b) receiver's aperture plane showing the far field intensity pattern at a certain instant with pointing error r_0

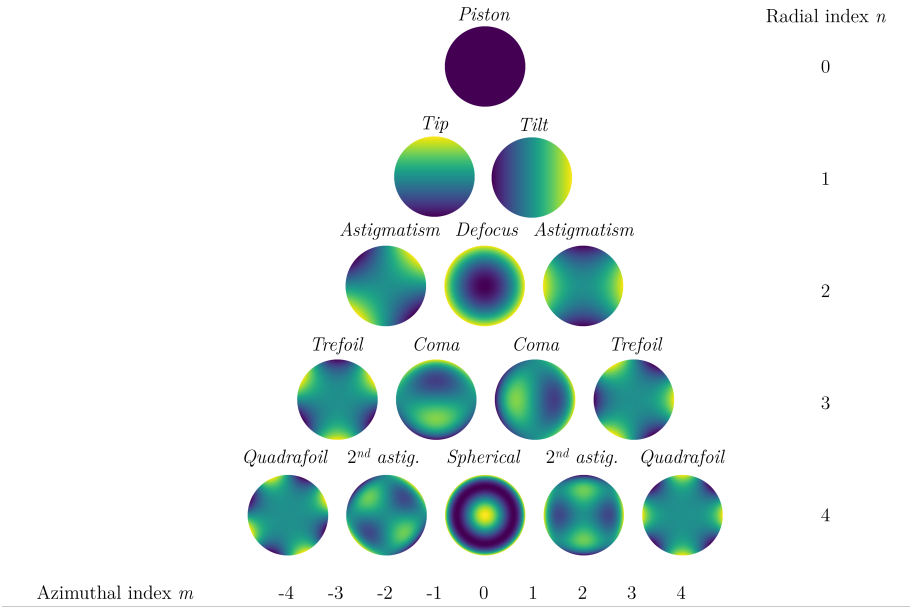

Figure 3. Zernike polynomials $Z_n^m(\rho, \varphi)$ for different radial and azimuthal indices, n and m respectively

performance of the system (comparing it to a completely static link). The received power as a function of the location of the center of the transmitted beam, given by the coordinates (x_0, y_0), with respect to the center of the receiver aperture can be computed through a bidimensional convolution of the receiver's aperture pupil and the far-field intensity at the receiver's aperture plane.

$$P = g(x_0, y_0) = \int\int_{R_{ap}} I(x, y)\, dxdy = \int\int_{\mathbb{R}^2} I(x, y)\, \mathcal{A}(x - x_0, y - y_0)\, dxdy \tag{5}$$

where $\mathcal{A}(x, y)$ is the pupil function of the receiver. As this work considers a symmetric intersatellite link, this pupil function is considered the same as for the transmitter (Equation 3). Using the convolution theorem, the received power as a function of (x_0, y_0) can be obtained from Equation 5 as

$$P = g(x_0, y_0) = \{I * \mathcal{A}\}(x_0, y_0) = \mathcal{F}^{-1}\{\mathcal{F}(I) \cdot \mathcal{F}(\mathcal{A})\} \tag{6}$$

The transmitter angular pointing jitter is usually characterized as a centered bivariate Gaussian distribution.[19–21] For the small angle approximation, it can be shown that this translates into a decenter error between the beam center and the receiver's axis given by a centered bivariate Gaussian distribution. Finally, considering that the standard deviation in x and y axes are the same (or in azimuth and elevation angles in the transmitter pointing), the pointing jitter can be described by the Rayleigh probability density function (PDF) given by

$$f_R(r_0) = \frac{r_0}{\sigma^2} \exp\left(-\frac{r_0^2}{2\sigma^2}\right) \tag{7}$$

where r_0 is the radial decenter (see Figure 2) and σ is the scale factor of the Rayleigh distribution*. For the nominal case, without wavefront errors, the far-field intensity distribution will be axially symmetric, and Equation 5 can be transformed from cartesian to polar coordinates as $g(x_0, y_0) \to g(r_0)$. When there are wavefront errors that break this symmetry (i.e. astigmatism or comma), the result in several axes is evaluated, as will be explained later.

What is needed to evaluate the performance of a communication system is the received power statistics. In this case, considering a slow fading channel (the modulation frequency of the communication signal is orders of

*This scale factor σ is the same as the standard deviation of the underlying symmetric bivariate Gaussian distribution

magnitude higher than the dynamics of the pointing jitter), the received power is characterized by a PDF. This PDF can be obtained by combining the power as a function of the displacement of the beam center $g(r_0)$ and the pointing jitter PDF, i.e. $f_R(r_0)$. The transformation between variables that are related by a non-monotonical function is

$$f_{\mathcal{P}}(P) = \sum_{k=1}^{n(P)} \left| \frac{d}{dP} g_k^{-1}(P) \right| \cdot f_R\big(g_k^{-1}(P)\big) \tag{8}$$

where $g_k^{-1}(P)$ is the k-th inverse function of $g(r_0)$.

2.3 Communication performance

Finally, the performance of the communication system can be evaluated with the Average Bit Error Probability (ABEP) as[22,23]

$$\text{ABEP} = \int_0^\infty P_e(e|h)\; f_{\mathcal{P}}(h)\; dh \tag{9}$$

where h is the received power normalized by the transmitted power (or channel loss) and the instantaneous conditioned bit error probability is

$$P_e(e|h) = Q^G\left(\sqrt{\text{SNR}}\right) \tag{10}$$

where $Q^G(x)$ is the Gaussian Q-function and the signal-to-noise ratio (SNR) for on-off keying intensity modulation direct detection (OOK IM/DD) is given by

$$\text{SNR} = \frac{2\left(hP_tR\right)^2}{\sigma_n^2} \tag{11}$$

where P_t is the transmitted power, R is the responsivity of the detector, and σ_n^2 is the signal independent additive white-Gaussian thermal noise.

3. RESULTS

Using the model presented above, the optimum nominal operation point is computed first by varying the beamwidth of the Gaussian in the aperture plane of the transmitter and the beamwaist of it. Then, the optical aberrations are included as a phase screen and the effect of each of them on the ABEP is computed. Table 1 shows the parameters chosen for the simulation.

Table 1. Parameters used for the simulations

Parameter	Value
λ	1550 nm
P_t	12 dBm
σ_n	4.7×10^{-9} V
σ_θ	10 μrad
z	1000 km
b	5 cm
a	1 cm

On an intersatellite scenario, given a pointing jitter σ, a distance z between the terminals, a transmitter power P_t, and a certain obscuration of the secondary mirror a/b, the optimum far-field irradiance pattern in the aperture of the receiver will be given by one that provides the minimum ABEP. There are different variables with which we can change the far-field irradiance distribution:

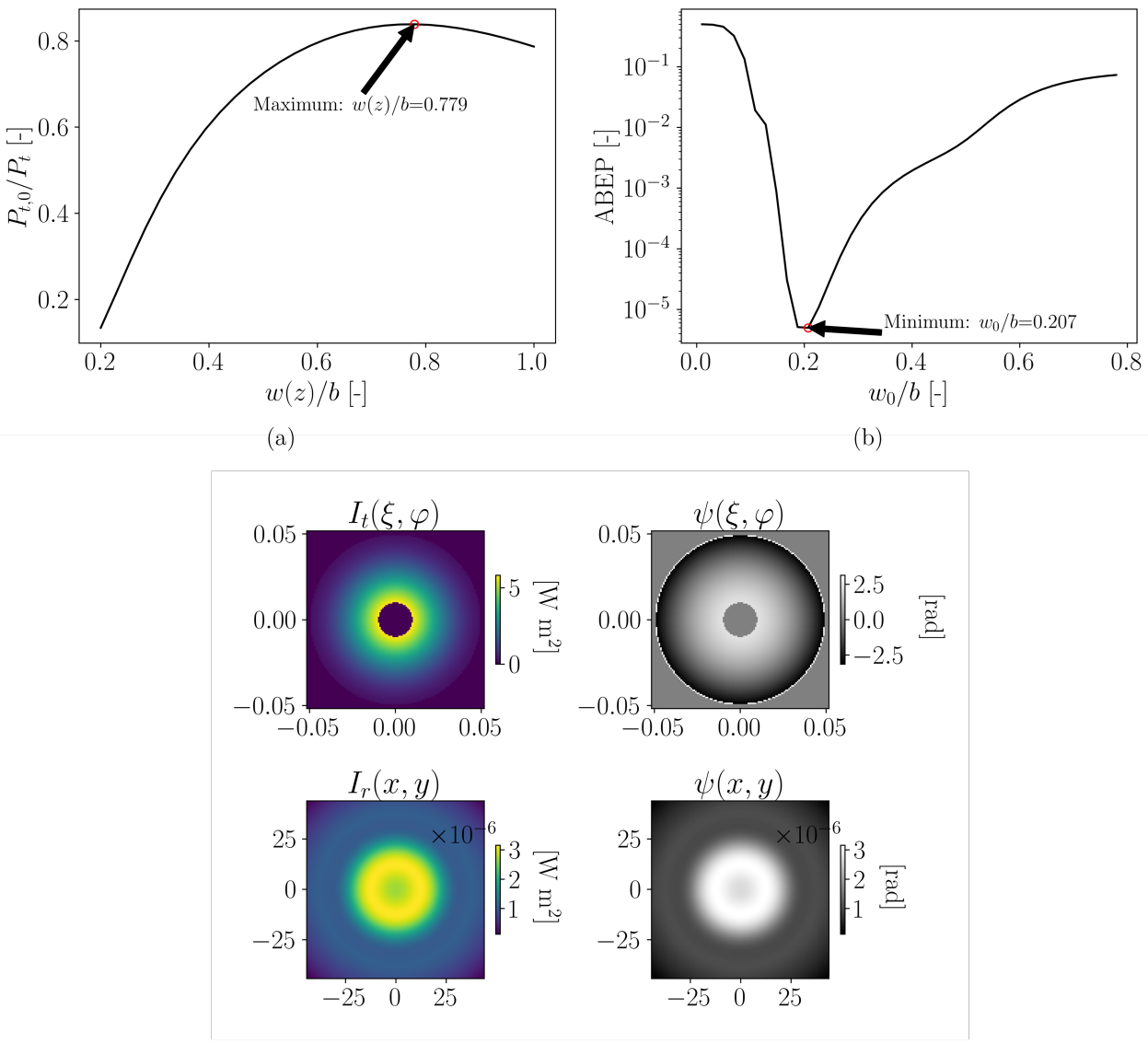

Figure 4. Nominal operation point of the intersatellite link, (a) power as a function of $w(z)/b$ in the transmitter's aperture plane, (b) ABEP as a function of w_0/b and (c) irradiance and phase fields on the transmitter and receiver aperture planes for $w(z)/b = 0.779$ and $w_0/b = 0.207$

1. Aperture size of the transmitter b.
2. Beam waist of the Gaussian beam w_0.
3. Clipping ratio $w(z)/b$ at the aperture of the receiver by defocusing the transmitted beam on the telescope.

By using these three parameters the far-field intensity distribution can be varied to find the optimum operational point for a given angular pointing jitter, link distance, and obscuration ratio. In this paper, to obtain the nominal link scenario [†], the aperture size of the transmitter will be set. As the intersatellite link that we are considering is symmetric, the aperture size plays a dual role in the performance of the system. On one side, it can be used

[†]nominal refers to the link without optical aberrations, just pointing jitter

to change the divergence of the transmitted beam (keeping the other two parameters constant). On the other side, the aperture size will also determine the amount of power collected by the receiver aperture. As the total transmitted power after the transmitter clipping occurs and the divergence of the beam can be adjusted using the other two parameters, the aperture of the transmitted will be settled at a certain value (see Table 1).

By adjusting the Gaussian beamwaist w_0 and the clipping ratio at the aperture $w(z)/b$ the power transmitted after the clipping and the divergence of the beam can be computed. In this case, the clipping ratio at the aperture $w(z)/b$ will be adjusted so that the power transmitted by the telescope after the clipping is maximum. This can be seen in Figure 4(a) where the power exiting the transmitter telescope $P_{t,0}$ as a function of the clipping is represented. Given the optimum $w(z)/b$ ratio for the obscuration ratio studied, the beam divergence can be adjusted by varying the beamwaist of the underlying Gaussian beam w_0[‡]. The optimum beam divergence will depend on the transmitter pointing jitter.[21] In Figure 4(b), the ABEP is shown as a function of the underlying Gaussian beam waist for the optimum $w(z)/b$ found in Figure 4(a). Taking the minimum ABEP, the nominal operation point is obtained, given by the values $w(z)/b = 0.779$ and $w_0/b = 0.207$. The irradiance and phase field on the transmitter aperture plane and the receiver aperture plane are shown in Figure 4(c).

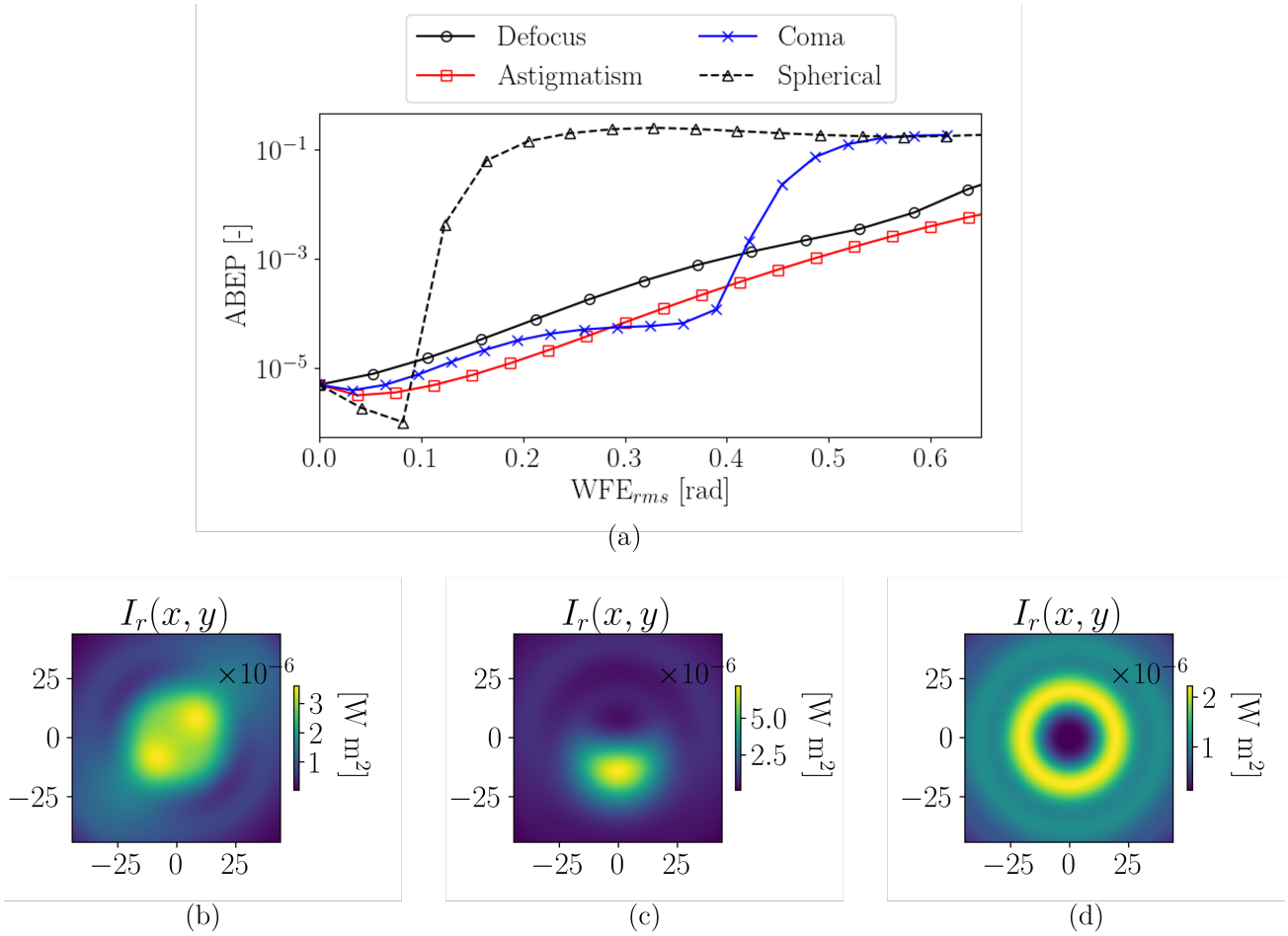

Figure 5. Impact of different optical aberrations in the communication performance of an intersatellite link, (a) ABEP as a function of the RMS value of the aberration and irradiance field on the receiver aperture plane for (b) astigmatism (c) coma and (d) spherical aberrations

From the nominal operating point shown in Figure 4, several aberrations have been added to the transmitted beam through the computational method explained above. Figure 5 shows the effect on the ABEP for different

[‡]In this paper, we will not deal with how this is done by optical design of the transmitter terminal

aberrations. The aberration is quantified by the root mean squared (RMS) of the distortion in the phase field created by it. As the divergence of the beam has been optimized through the variation of w_0/b further defocus of the beam will deteriorate the performance of the system as it is seen in Figure 5. Astigmatism and coma aberrations do not have azimuthal symmetry so the computational model explained above can not be directly used. To compute the effect of each of these aberrations, their horizontal and vertical modes (see Figure 3) have been averaged. Finally, the spherical aberration has been investigated, and a very interesting result has been obtained. Indeed a slight a spherical aberration, changes the far-field irrandiance pattern in such a way that the system performance is improved. However, further increase of the spherical aberration will rapidly degrade the performance of the system.

4. CONCLUSIONS

A computational model is presented to compute the impact of optical aberrations occurring on the transmitter of an intersatellite free space optical communication link. The model uses computational Fourier optics to obtain the far-field irradiance pattern on the receiver's aperture plane. By computing the power statistics given by this irradiance field under pointing jitter, the communication performance of the system is evaluated by the average bit error probability. Using this model, the optimum nominal link parameters are obtained by varying the beamwidth at the transmitter's aperture plane and the beamwaist of the Gaussian beam. Then, several aberrations are added to the system and their impact on the communication performance is computed by evaluating the resulting average bit error probability. The results show similar performance-degrading effects for defocus, astigmatism, and coma. For spherical aberration, a slight improvement can be seen for small values of the aberration. The latter is due to a better distribution of the irradiance in the far field compared to the nominal case.

ACKNOWLEDGMENTS

The authors would like to thank the support from the Dutch Research Council (NWO) for funding the Perspectief Project P19-13 "Optical Wireless Super Highways"

REFERENCES

[1] Khatri, S., Brady, A. J., Desporte, R. A., Bart, M. P., and Dowling, J. P., "Spooky action at a global distance: analysis of space-based entanglement distribution for the quantum internet," *npj Quantum Information* **7**, 1–15 (Jan. 2021).

[2] Liorni, C., Kampermann, H., and Bruß, D., "Quantum repeaters in space," *New Journal of Physics* **23**, 053021 (May 2021).

[3] Wallnöfer, J., Hahn, F., Gündoğan, M., Sidhu, J. S., Wiesner, F., Walk, N., Eisert, J., and Wolters, J., "Simulating quantum repeater strategies for multiple satellites," *Communications Physics* **5**, 1–8 (June 2022).

[4] Badás, M., Piron, P., Bouwmeester, J., Loicq, J., Kuiper, H., and Gill, E., "Opto-thermo-mechanical phenomena in satellite free-space optical communications: survey and challenges," *Optical Engineering* **63**, 041206 (Oct. 2023).

[5] Toyoshima, M., "Maximum fiber coupling efficiency and optimum beam size in the presence of random angular jitter for free-space laser systems and their applications," *JOSA A* **23**, 2246–2250 (Sept. 2006).

[6] Ma, J., Zhao, F., Tan, L., Yu, S., and Yang, Y., "Degradation of single-mode fiber coupling efficiency due to localized wavefront aberrations in free-space laser communications," *Optical Engineering* **49**, 045004 (Apr. 2010).

[7] Toyoshima, M., Takahashi, N., Jono, T., Yamawaki, T., Nakagawa, K., and Yamamoto, A., "Mutual alignment errors due to the variation of wave-front aberrations in a free-space laser communication link," *Optics Express* **9**, 592–602 (Nov. 2001).

[8] Sun, J., Liu, L., Yun, M., and Wan, L., "Mutual alignment errors due to wave-front aberrations in intersatellite laser communications," *Applied Optics* **44**, 4953–4958 (Aug. 2005).

[9] Yang, Y., Tan, L., and Ma, J., "Mutual alignment errors due to localized distortion in free-space laser communication links," *Optics Communications* **281**, 4180–4187 (Sept. 2008).

[10] Tan, L., Yang, Y., Ma, J., and Yu, J., "Pointing and tracking errors due to localized deformation in inter-satellite laser communication links," *Optics Express* **16**, 13372–13380 (Aug. 2008).

[11] Yang, Y., Tan, L., and Ma, J., "Pointing and tracking errors due to localized distortion induced by a transmission-type antenna in intersatellite laser communications," *Applied Optics* **48**, 786–791 (Feb. 2009).

[12] Yang, Y., Tan, L., Ma, J., and Yu, J., "Effects of localized deformation induced by reflector antenna on received power," *Optics Communications* **282**, 396–400 (Feb. 2009).

[13] Xie, W., Tan, L., Ma, J., Yang, Y., and Ran, Q., "Received power analysis due to antenna deformation based on wavelet in inter-satellite laser communication links," *Optik* **123**, 670–674 (Apr. 2012).

[14] Yang, Y., Cao, G., and Zhao, H., "Influence of localized distortion in lenses on Strehl ratio in lasercom," *Optik* **124**, 6415–6418 (Dec. 2013).

[15] Yang, Y., Han, Q., Tan, L., Ma, J., Yu, S., Yan, Z., Yu, J., and Zhao, S., "Influence of wave-front aberrations on bit error rate in inter-satellite laser communications," *Optics Communications* **284**, 3065–3069 (June 2011).

[16] Yang, Y., Han, Q., Tan, L., and Zhang, G., "Research on Bit Error Rate in the Presence of Local Wavefront Aberration in Intersatellite Laser Communications," *Journal of Lightwave Technology* **29**, 2893–2898 (Oct. 2011).

[17] Goodman, J. W., [*Introduction to Fourier optics*], Roberts & Co., Englewood, Colo., 3rd ed ed. (2005).

[18] Niu, K. and Tian, C., "Zernike polynomials and their applications," *Journal of Optics* **24**, 123001 (Nov. 2022).

[19] Song, T., Wang, Q., Wu, M.-W., Ohtsuki, T., Gurusamy, M., and Kam, P.-Y., "Impact of Pointing Errors on the Error Performance of Intersatellite Laser Communications," *Journal of Lightwave Technology* **35**, 3082–3091 (July 2017).

[20] Zaman, I. U. and Boyraz, O., "Impact of receiver architecture on small satellite optical link in the presence of pointing jitter," *Applied Optics* **59**, 10177–10184 (Nov. 2020).

[21] Toyoshima, M., Jono, T., Nakagawa, K., and Yamamoto, A., "Optimum intersatellite link design in the presence of random pointing jitter for free-space laser communication systems," in [*Free-Space Laser Communication Technologies XIV*], **4635**, 95–102, SPIE (Apr. 2002).

[22] Yang, F., Cheng, J., and Tsiftsis, T. A., "Free-Space Optical Communication with Nonzero Boresight Pointing Errors," *IEEE Transactions on Communications* **62**, 713–725 (Feb. 2014).

[23] Do, P. X., Carrasco-Casado, A., Vu, T. V., Hosonuma, T., Toyoshima, M., and Nakasuka, S., "Numerical and analytical approaches to dynamic beam waist optimization for LEO-to-GEO laser communication," *OSA Continuum* **3**, 3508–3522 (Dec. 2020).